Letter

Stretchable Kirigami Polyvinylidene Difluoride Thin Films for Energy Harvesting: Design, Analysis, and Performance

Nan Hu,[1,2] Dajing Chen,[1,3] Dong Wang,[1,4] Shicheng Huang,[1] Ian Trase,[1] Hannah M. Grover,[1] Xiaojiao Yu,[1] John X. J. Zhang,[1,*] and Zi Chen[1,†]

[1]*Thayer School of Engineering, Dartmouth College, Hanover, New Hampshire 03755, USA*
[2]*Department of Civil, Environmental and Geodetic Engineering, The Ohio State University, Columbus, Ohio 43210, USA*
[3]*Medical School, Hangzhou Normal University, Hangzhou, Zhejiang 311121, China*
[4]*The Science Cluster, Singapore University of Technology and Design, 487372 Singapore, Singapore*

(Received 28 April 2017; revised manuscript received 2 November 2017; published 22 February 2018)

Kirigami, a modified form of origami which includes cutting, has been used to improve material stretchability and compliance. However, this technique is, so far, underexplored in patterning piezoelectric materials towards developing efficient and mechanically flexible thin-film energy generators. Motivated by existing kirigami-based applications, we introduce interdigitated cuts to polyvinylidene fluoride (PVDF) films to evaluate the effect on voltage generation and stretchability. Our results from theoretical analysis, numerical simulations, and experimental tests show that kirigami PVDF films exhibit an extended strain range while still maintaining significant voltage generation compared to films without cuts. Various cutting patterns are studied, and it is found that films with denser cuts have a larger voltage output. This kirigami design can enhance the properties of existing piezoelectric materials and help to integrate tunable PVDF generators into biomedical devices.

DOI: 10.1103/PhysRevApplied.9.021002

Kirigami, a variation of origami that introduces cutting, can create complex 3D geometries from flat 2D sheets through out-of-plane deformations. A wide range of technologies have been inspired by kirigami [1]. At the nanoscale, kirigami has enabled the shape formation and self-assembly of 3D nanostructures from 2D sheets. Examples include DNA nanotechnology [2], nanomembranes [3], and nanoelectromechanical systems [4]. Blees *et al.* [5] designed kirigami graphene sheets to achieve large ductility and resilience for stretchable electronics and photovoltaics. Based upon this work, the introduction of kirigami molybdenum disulfide has significantly increased yield and fracture strains [6]. Similarly, Shyu *et al.* [7] created kirigami nanocomposites that can extend ultimate strain up to 370%. At larger scales, kirigami has inspired novel designs in biosensing [8], steering mechanisms [9], cellular metamaterials [10], reconfigurable metamaterials [11], bioprobe devices [12], stretchable lithium-ion batteries [13], solar tracking systems [14], adaptive morphing wings [15], energy dissipation structures [16], and energy-efficient building skins [17]. While most studies focus on modifying geometry and morphology to achieve high stretchability [18], there has been a recent emphasis on mechanical instability related to origami and kirigami. Mechanical instabilities can be a favorable phenomenon for smart materials [19], and stimuli responsive systems [20,21]. For example, 3D microstructures and nanostructures were fabricated via the compressive buckling of filamentary ribbons, whose tunable geometric features enabled the rapid assembly of stimuli responsive structures [22].

In this Letter, we use kirigami to improve the ability of piezoelectric materials to act as a power source for portable and implantable devices. In recent years, several flexible, stretchable devices have been developed for energy harvesting [23], self-power generation [24], spatiotemporal cardiac measurements [25], motion detection of fingers [26], wearable electronic devices [27], and high-strain sensors [28]. Among the many types of piezoelectric materials, polyvinylidene fluoride (PVDF) is the most promising for biomedical applications due to its low cost, light weight, mechanical performance, and excellent biocompatibility. Current PVDF-based devices are mostly 2D structures, limited to in-plane deformation. Our previous studies on PVDF films have demonstrated their potential for energy generation [29] with both symmetric and asymmetric pore distribution [30]. Porous PVDF films, for example, have enabled a new generation of minimally invasive glucose sensors [31]. We introduce patterned cuts on PVDF films to induce out-of-plane deformation. The hypothesis is that kirigami can increase the strain range of piezoelectric

*Corresponding author.
john.zhang@dartmouth.edu
†Corresponding author.
zi.chen@dartmouth.edu

 © 2018 American Physical Society

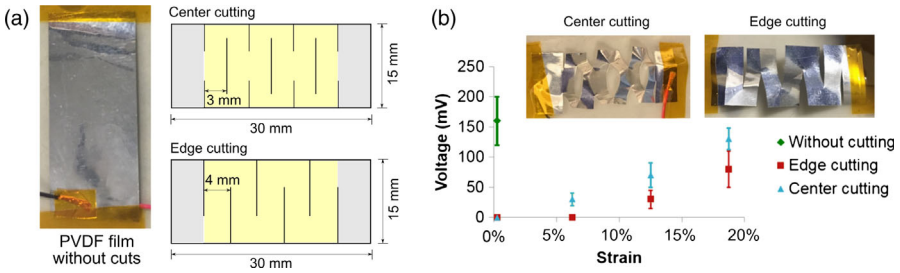

FIG. 1. The design and performance of kirigami PVDF films. (a) Baseline film without cuts and kirigami patterns. (b) Piezoelectric output between PVDF films with and without cuts.

structures while still maintaining significant energy generation. We envision that the tunability of kirigami can be applied to multifunctional piezoelectric devices such as biomedical devices.

As a proof of concept, we began by fabricating baseline solid PVDF films (see the Supplemental Material [32]). Figure 1(a) shows a thin film 30 mm long, 15 mm wide, and 50 μm thick. The 200-nm-thick electrodes are deposited on the PVDF layer (25 μm) by an *E*-beam evaporator. The bottom Kapton film, with a thickness of 25 μm, is used as a supporting substrate to increase the stiffness of the specimen. We use a scalpel to cut the baseline PVDF films with two different patterns, center cutting and edge cutting. It should be noted that noncutting regions of 6 mm are reserved on each end of the PVDF film for an electrical connection to measurement circuitry. As a result, cuts are only applied to the middle portion of the film (18 mm). The center-cutting design has the cut length of 10 mm in the center and 5 mm on the edge, while the edge-cutting design contains only 10-mm-long cuts along the edge. PVDF films with both cutting patterns are uniaxially stretched with a motorized test stage. The maximum load (0.75 N) is set constant, since the piezoelectric output is directly related to the stress applied. We put a force gauge at one end of the kirigami structure during testing. A load-limiting test is used, as the moving stage will automatically stop once it reaches the maximum load.

After measuring the voltage output through the charge amplifier, we compare the performance of PVDF films with and without cuts. Figure 1(b) shows the deformed shape of the two cutting patterns. The strain in our experiment is an effective strain, defined as the elongation divided by the original length. As expected, the PVDF film without cuts has a larger voltage output (160 mV) yet a smaller strain (1%). Kirigami-based PVDF films, in contrast, attain a slightly smaller voltage output but can attain strains of up to 18% without fracture. Note that the film with the center-cutting pattern has a larger voltage output (132 mV) than the one with the edge-cutting pattern (85 mV). The main contributor to the voltage output is the stress due to the in-plane surface stretching of the film. The center-cutting design has a larger portion of surface area under tensile stress during the stretching process, so it has a larger voltage output.

We characterized the response of the center-cut PVDF under axial stretching using finite element (FE) software (ABAQUS, standard version 6.14), as shown in Video 1(a). The kirigami PVDF films are designed in SOLIDWORKS and then imported to ABAQUS. The 3D solid geometry of the PVDF film is meshed with the C3D20RE element type and the Kapton film is meshed with the C3D20R element type. We do not include the aluminum layers due to the less significant thickness (200 nm) compared to the thicknesses of the PVDF and Kapton layers. The Young's modulus of

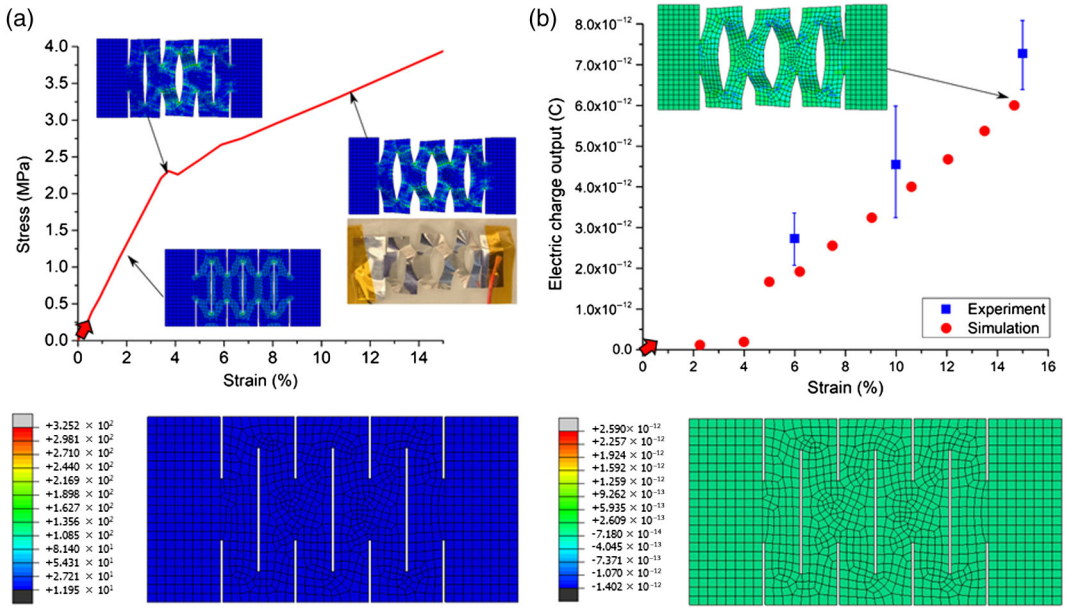

VIDEO 1. Simulation of kirigami PVDF films under axial stretching. (a) Stress-strain curve for a PVDF film with center cuts. (b) Comparison of electric charges in PVDF film with center cutting between experiment and simulation.

the PVDF film is 1.53 GPa and the Poisson's ratio is 0.37. The dielectric constant of the PVDF film is 1.06×10^{-10} and its piezoelectric properties d_{31} and d_{33} are -21×10^{-12} C/N and -29×10^{-12} C/N, respectively. The Young's modulus of the Kapton film is 2.5 GPa and the Poisson's ratio is 0.34. An axial load is applied at one end while a clamped condition is applied at the other. Simulations are performed using a dynamic implicit solver. A synchronized video featuring the stress-strain curve and charge-strain curve is shown in Video 1. Video 1(a) shows two regimes in the force-displacement curve divided by a critical buckling load. Prior to the critical point, the film only undergoes in-plane deformation. A drop in force is observed after the critical point, indicating the onset of out-of-plane deformation. Numerically, the buckling of the film is triggered due to the asymmetric mesh of the computational model. The load magnitude then increases linearly as the stretching process continues. Excellent deformed shape agreement is found between experiments and finite element simulations. The von Mises stress is defined as

$$\sigma_{\mathrm{VM}} = \sqrt{[(\sigma_{11}-\sigma_{22})^2 + (\sigma_{22}-\sigma_{33})^2 + (\sigma_{33}-\sigma_{11})^2]/2 + 3(\tau_{12}^2 + \tau_{23}^2 + \tau_{13}^2)},$$

where σ_{11}, σ_{22}, σ_{33} are normal stresses and τ_{12}, τ_{23}, τ_{13} are shear stresses, which is widely used to predict the yielding of materials under complex loading. Here, the distributions of the von Mises stress from the simulation are plotted as insets in Video 1(a). It can be seen that a higher von Mises stress (lighter color) is observed at sharp corners of cuts, which does limit the stretchability of the film. In fact, a recent study [7] has found that the kirigami structures can be further stretched after introducing rounded edges at these sharp corners. Thus, the investigation on the stress redistribution and optimization of the kirigami PVDF is beyond the scope of this work.

We further validate the accuracy of our numerical model by comparing the charge output obtained from the experiment and the estimated charge output from the numerical model, see Video 1(b). The experimental value of the electric charge is calculated by $Q = C(V/A_{\mathrm{VD}})$, where C is the feedback capacitor used in the charge amplifier (10×10^{-9} F); V is the voltage measured by charge amplifier; and A_{VD} is the amplifier voltage gain (110 V). For example, the electric charge when the measured voltage at 6% strain (22 mV) is 2.00×10^{-12} C while the simulated charge is 1.92×10^{-12} C. In the simulation, we request a total of ten data points to show the changing of the total charge within the film. It can be seen that after the film buckles at 4% strain, a significant jump is observed in the total electric charge output. The simulated electric charge is less than those experimental data, but the error between experiment and simulation is acceptable.

We have demonstrated that kirigami PVDF films have an increased strain range without a significant loss in voltage output. We further explored center-cutting kirigami patterns to improve the voltage output and strain range of PVDF films. Shyu *et al.* [7] evaluated the effect of different cuts on film stretchability and found that longitudinal cuts have the most significant influence on maximum strain. Isobe and Okumura conducted an analysis to predict the stiffness and the critical stretching strain of a kirigami film [33]. Based on their work, we further develop theoretical analysis (see the Supplemental Material [32]) and run finite element simulations to study three kirigami designs with different cut spacing in the longitudinal direction, as shown in Fig. 2(a). These three films have an equal length (60 mm) and width (15 mm). The first sample has cuts spaced every 2 mm, while a second has cuts spaced every 4 mm. The third film is a hybrid of both cuts, having 2-mm spaces in one segment and 4-mm spaces in the other. All three films are stretched in their elastic regimes without

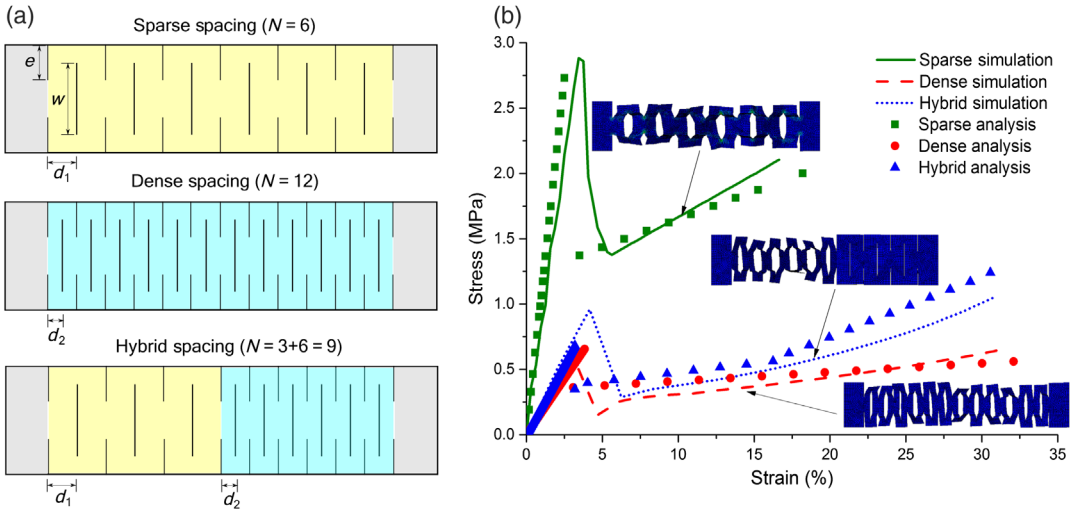

FIG. 2. The effect of kirigami pattern. (a) Pattern designs. (b) Comparison between the stress-strain curves from simulations (lines) with theoretical predictions (scattered points).

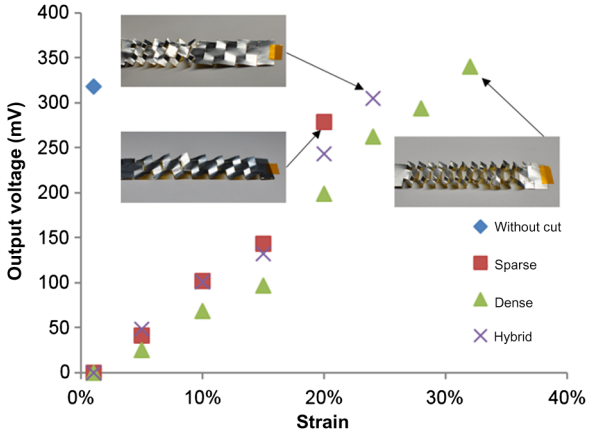

FIG. 3. Measured voltage output and strain for different cutting patterns. Inset: deformed configuration of kirigami PVDF film after stretching.

considering material damage. We plot the stress vs strain curve of the hybrid cut design and two single-cut designs in Fig. 2(b). The response of a kirigami film transitions between two regimes: in-plane and out-of-plane deformation. In the hybrid design, the dense segment (2 mm) moves into the postbuckling, out-of-plane regime before the sparse segment (4 mm). At this point, the sparse-spacing segment is not fully stretched due to a large stress concentration at the interface between two segments. In Fig. 2(b) we plot the theoretical analysis as scatter points to compare with the numerical simulation results. A good agreement between simulation and theoretical analysis is observed.

We fabricate the above-mentioned films along with a baseline design without cuts and measure their voltage outputs through a charge amplifier (Fig. 3). These new films have a total length of 60 mm rather than the 30 mm of previous films. The voltage output of the PVDF film without cuts (325 mV) in the 60-mm-long film is double that of the previous 30-mm-long film (160 mV). The cut lengths stay the same as those in Fig. 1. As we stretch the films with cuts to about 20% strain, the dense design has a larger voltage output (283 mV) than both the hybrid design and the sparse design. At 20% strain the sparsely cut film is fully stretched, and we observe larger strain limits for both the hybrid design (24%) and the dense design (33%). This stretchability is above the general upper limit for skin (20%). The voltage output (296 mV) associated with the hybrid design is approximately the same as the one without cuts, while the voltage output (333 mV) of the dense design even exceeds the cut-free film. This phenomenon is similar to the one we observe in Fig. 1, the underlying reason of which is that the main contributor to the voltage output is the stress due to the in-plane surface stretching of the film. In the sparse design, the film is limited by the stress distribution at those sharp corners, which in turn cause a lower stress on the other locations of the film surface. The denser design has a higher stress at other locations of the film, which leads to a higher voltage generation.

Among the patterns, the dense design has the largest number of cuts and sharp corners, and has the largest voltage output, which might indicate a correlation between these two parameters. The hybrid design is not fully stretched, as we observe cracks at the interface between the dense and the sparse portions of the film. Other designs also have the same damage at sharp corners. We also test performance when the film is subjected to several stretching cycles. The dense design has a mean average of 340 mV for the voltage output but becomes damaged after five loading cycles. If we stretch the same film at a strain level 5% less than the limit of 33%, the voltage output remains at 299 mV without any damage.

In summary, we introduce interdigitated and other patterned cuts on PVDF thin films to enhance energy generation ability. Supported by theoretical analysis, FE simulations, and experiments, we show that axially stretched kirigami PVDF films can attain a much higher strain limit (30%) while maintaining the same level of voltage output compared to regular PVDF films. The current designs can be extended beyond the component level, towards the exploration of biaxial stretching and 3D system assembly. As high strains will likely be observed in the potential design of wearable and implantable devices (such as electronic clothes and finger posture detection), piezoelectric PVDF-trifluoroethylene films, in combination with a careful design of supporting mechanical membranes, can be used to make flexible devices. We believe the concept of kirigami-patterned functional thin films can also be applied to other types of energy harvesters such as patch-based thin plates [34] and origami-based structures [35]. State-of-the-art piezoelectric polymer-based devices rely on thin-film geometries. These conventional devices have been intensively studied but have not proven capable of achieving sufficiently high voltage output. Our study shows that kirigami-based piezoelectric materials can enhance piezoelectric output with extended stress-strain responses for high-efficiency power generation devices. We envision a promising future in which kirigami-based piezoelectric materials are fully adapted into self-powered biomedical devices.

Note: Dartmouth College has filed a patent application relating to the use of kirigami structures for energy harvesting based on the results of this study.

ACKNOWLEDGMENTS

Z. C. acknowledges the startup fund from the Thayer School of Engineering at Dartmouth and the support from the Branco Weiss–Society in Science Fellowship, administered by ETH Zürich. X. J. Z. acknowledges the support from the NIH Director's Transformative Research Award (No. R01HL137157), and NSF Grants No. ECCS 1128677, No. 1309686, and No. 1509369. We gratefully acknowledge the support from the Microfabrication and Electron

Microscope Facility at Dartmouth College. N. H. acknowledges the startup fund from the College of Engineering at The Ohio State University.

N. H. and D. C. contributed equally to this work.

[1] G. P. Collins, Science and culture: Kirigami and technology cut a fine figure, together, Proc. Natl. Acad. Sci. U.S.A. **113**, 240 (2016).
[2] D. Han, S. Pal, Y. Liu, and H. Yan, Folding and cutting DNA into reconfigurable topological nanostructures, Nat. Nanotechnol. **5**, 712 (2010).
[3] F. Cavallo and M. G. Lagally, Nano-origami: Art and function, Nano Today **10**, 538 (2015).
[4] Z. Chen, G. Huang, I. Trase, X. Han, and Y. Mei, Mechanical Self-Assembly of a Strain-Engineered Flexible Layer: Wrinkling, Rolling, and Twisting, Phys. Rev. Applied **5**, 017001 (2016).
[5] M. K. Blees, A. W. Barnard, P. A. Rose, S. P. Roberts, K. L. McGill, P. Y. Huang, A. R. Ruyack, J. W. Kevek, B. Kobrin, D. A. Muller, and P. L. McEuen, Graphene kirigami, Nature (London) **524**, 204 (2015).
[6] P. Z. Hanakata, Z. Qi, D. K. Campbell, and H. S. Park, Highly stretchable MoS_2 kirigami, Nanoscale **8**, 458 (2016).
[7] T. C. Shyu, P. F. Damasceno, P. M. Dodd, A. Lamoureux, L. Xu, M. Shlian, M. Shtein, S. C. Glotzer, and N. A. Kotov, A kirigami approach to engineering elasticity in nanocomposites through patterned defects, Nat. Mater. **14**, 785 (2015).
[8] L. Xu, X. Wang, Y. Kim, T. C. Shyu, J. Lyu, and N. A. Kotov, Kirigami nanocomposites as wide-angle diffraction gratings, ACS Nano **10**, 6156 (2016).
[9] W. Wang, C. Li, H. Rodrigue, F. Yuan, M.-W. Han, M. Cho, and S.-H. Ahn, Kirigami/origami-based soft deployable reflector for optical beam steering, Adv. Funct. Mater. **27**, 1604214 (2017).
[10] M. Eidini and G. H. Paulino, Unraveling metamaterial properties in zigzag-base folded sheets, Sci. Adv. **1**, e1500224 (2015).
[11] A. Rafsanjani and K. Bertoldi, Buckling-Induced Kirigami, Phys. Rev. Lett. **118**, 084301 (2017).
[12] Y. Morikawa, S. Yamagiwa, H. Sawahata, M. Ishida, and T. Kawano, in *Proceedings of the 2016 IEEE 29th International Conference on Micro Electro Mechanical Systems (MEMS)* (IEEE, New York, 2016), p. 149.
[13] Z. Song, X. Wang, C. Lv, Y. An, M. Liang, T. Ma, D. He, Y.-J. Zheng, S.-Q. Huang, H. Yu, and H. Jiang, Kirigami-based stretchable lithium-ion batteries, Sci. Rep. **5**, 10988 (2015).
[14] A. Lamoureux, K. Lee, M. Shlian, S. R. Forrest, and M. Shtein, Dynamic kirigami structures for integrated solar tracking, Nat. Commun. **6**, 8092 (2015).
[15] K. Saito, F. Agnese, and F. Scarpa, A cellular kirigami morphing wingbox concept, J. Intell. Mater. Syst. Struct. **22**, 935 (2011).
[16] Y. Hou, R. Neville, F. Scarpa, C. Remillat, B. Gu, and M. Ruzzene, Graded conventional-auxetic Kirigami sandwich structures: Flatwise compression and edgewise loading, Composites Part B **59**, 33 (2014).
[17] Y. Tang, G. Lin, S. Yang, Y. K. Yi, R. D. Kamien, and J. Yin, Programmable Kiri-Kirigami Metamaterials, Adv. Mater. **29**, 1604262 (2017).
[18] D. M. Sussman, Y. Cho, T. Castle, X. Gong, E. Jung, S. Yang, and R. D. Kamien, Algorithmic lattice kirigami: A route to pluripotent materials, Proc. Natl. Acad. Sci. U.S.A. **112**, 7449 (2015).
[19] N. Hu and R. Burgueño, Buckling-induced smart applications: Recent advances and trends, Smart Mater. Struct. **24**, 063001 (2015).
[20] Z. Chen, Q. Guo, C. Majidi, W. Chen, D. J. Srolovitz, and M. P. Haataja, Nonlinear Geometric Effects in Mechanical Bistable Morphing Structures, Phys. Rev. Lett. **109**, 114302 (2012).
[21] Q. Guo, A. K. Mehta, M. A. Grover, W. Chen, D. G. Lynn, and Z. Chen, Shape selection and multi-stability in helical ribbons, Appl. Phys. Lett. **104**, 211901 (2014).
[22] S. Xu *et al.*, Assembly of micro/nanomaterials into complex, three-dimensional architectures by compressive buckling, Science **347**, 154 (2015).
[23] Y. Qi, J. Kim, T. D. Nguyen, B. Lisko, P. K. Purohit, and M. C. McAlpine, Enhanced piezoelectricity and stretchability in energy harvesting devices fabricated from buckled PZT ribbons, Nano Lett. **11**, 1331 (2011).
[24] W. Wu, S. Bai, M. Yuan, Y. Qin, Z. L. Wang, and T. Jing, Lead zirconate titanate nanowire textile nanogenerator for wearable energy-harvesting and self-powered devices, ACS Nano **6**, 6231 (2012).
[25] L. Xu *et al.*, 3D multifunctional integumentary membranes for spatiotemporal cardiac measurements and stimulation across the entire epicardium, Nat. Commun. **5**, 3329 (2014).
[26] M. Amjadi, A. Pichitpajongkit, S. Lee, S. Ryu, and I. Park, Highly stretchable and sensitive strain sensor based on silver nanowire–elastomer nanocomposite, ACS Nano **8**, 5154 (2014).
[27] J. T. Muth, D. M. Vogt, R. L. Truby, Y. Mengüç, D. B. Kolesky, R. J. Wood, and J. A. Lewis, Embedded 3D printing of strain sensors within highly stretchable elastomers, Adv. Mater. **26**, 6307 (2014).
[28] C. Yan, J. Wang, W. Kang, M. Cui, X. Wang, C. Y. Foo, K. J. Chee, and P. S. Lee, Highly stretchable piezoresistive graphene–nanocellulose nanopaper for strain sensors, Adv. Mater. **26**, 2022 (2014).
[29] D. Chen, T. Sharma, and J. X. J. Zhang, Mesoporous surface control of PVDF thin films for enhanced piezoelectric energy generation, Sens. Actuators A **216**, 196 (2014).
[30] D. Chen and J. X. J. Zhang, Microporous polyvinylidene fluoride film with dense surface enables efficient piezoelectric conversion, Appl. Phys. Lett. **106**, 193901 (2015).
[31] D. Chen, C. Wang, W. Chen, Y. Chen, and J. X. J. Zhang, PVDF-Nafion nanomembranes coated microneedles for *in vivo* transcutaneous implantable glucose sensing, Biosens. Bioelectron. **74**, 1047 (2015).
[32] See Supplemental Material at http://link.aps.org/supplemental/10.1103/PhysRevApplied.9.021002 for the key fabrication steps of PVDF films, theoretical derivation of films with hybrid pattern, and a movie of simulated

stress-strain response and electric charge output for a PVDF film with center cutting.

[33] M. Isobe and K. Okumura, Initial rigid response and softening transition of highly stretchable kirigami sheet materials, Sci. Rep. **6**, 24758 (2016).

[34] B. Bayik, A. Aghakhani, I. Basdogan, and A. Erturk, Equivalent circuit modeling of a piezo-patch energy harvester on a thin plate with AC-DC conversion, Smart Mater. Struct. **25**, 055015 (2016).

[35] P.-K. Yang, Z.-H. Lin, K. C. Pradel, L. Lin, X. Li, X. Wen, J.-H. He, and Z. L. Wang, Paper-based origami triboelectric nanogenerators and self-powered pressure sensors, ACS Nano **9**, 901 (2015).